Available online at www.sciencedirect.com

ScienceDirect

Advances in Space Research xxx (2020) xxx–xxx

ADVANCES IN SPACE RESEARCH (a COSPAR publication)

www.elsevier.com/locate/asr

The update of BDS-2 TGD and its impact on positioning

Yize Zhang [a,b], Junping Chen [a,*], Xiuqiang Gong [a], Qian Chen [a]

[a] Shanghai Astronomical Observatory, Shanghai 200030, China
[b] Tokyo University of Marine Science and Technology, Tokyo 1358533, Japan

Received 12 November 2019; received in revised form 5 March 2020; accepted 9 March 2020

Abstract

Timing group delay (TGD) is an important parameter that affects the positioning performance of global navigation satellite systems (GNSS). The BeiDou navigation satellite system (BDS) broadcasts TGD corrections from B3I frequency to B1I and B2I frequencies, namely TGD_1 and TGD_2. On July 21, 2017, BDS updated TGD values with a maximum change of more than 4 ns. In this contribution, we explain the motivation for the BDS TGD update, which is due to the systematic bias between narrowly correlated and widely correlated pseudo-ranges in BDS monitoring receivers. To investigate the impact of the updated TGD, BDS signal-in-space range error (SISRE) and user positioning performance regarding single point positioning (SPP) and precise point positioning (PPP) are analyzed. Results show that after the update of TGD, the difference between the new TGD and multi-GNSS experiment (MGEX) differential code bias (DCB) decreases from 1.38 ns to 0.29 ns on TGD_1 and from 0.40 ns to 0.25 ns on TGD_2. With the contribution of more accurate TGD, the systematic bias of BDS radial SISRE no longer exists, and the overall BDS SISRE also reduces from 1.33 m to 0.87 m on B1I/B2I frequency, from 1.05 m to 0.89 m on B1I frequency, from 0.92 m to 0.91 m on B2I frequency, respectively, which proves the similar precision of BDS TGD and MGEX DCB. One week of statistical results from 28 globally distributed MGEX stations shows that the SPP performance improves on non-B3I frequencies after the TGD update, with a maximum improvement of more than 22% for the B1I/B2I or B1I/B3I combination. The new TGD mainly reduces SPP positioning bias in the East component. The updated TGD also slightly improves the PPP convergence performance for the B1I/B3I combination, but mostly contributes to a more accurate estimation of the receiver clock and ambiguities.

Keywords: Timing group delay; Differential code bias; Signal-in-space range error; Single point positioning; Precise point positioning

1. Introduction

The BeiDou navigation satellite system (BDS), together with GPS, GLONASS, and Galileo, has become one of the global navigation satellite systems (GNSS). Since the official service started in late 2012, the basic positioning performance of the second phase of BDS (BDS-2) is promised to be better than 10 m in Asia-Pacific regional areas, covering latitudes 55°S to 55°N and longitudes 70°E to 150°E (CSNO, 2016; Yang et al., 2014). With the development of the third phase of BDS (BDS-3), BDS will provide a global and superior positioning, navigation and timing (PNT) service by the end of 2020, thanks to the better position dilution of precision (PDOP) and more precise satellite orbit and clock due to the inter-satellite link (ISL) and more stable Rubidium and passive hydrogen maser clock (Tang et al., 2018; Zhang et al., 2018; Wu et al., 2018; Yang et al., 2018; Yang et al., 2019).

GNSS signals are affected by satellite- and receiver-introduced instrumental delay, which is usually called timing group delay (TGD) or differential code bias (DCB) (Guo et al., 2015; Håkansson et al., 2017). The clock broadcast in the navigation ephemeris and the real-time

* Corresponding author.
E-mail address: junping@shao.ac.cn (J. Chen).

https://doi.org/10.1016/j.asr.2020.03.011
0273-1177/© 2020 Published by Elsevier Ltd on behalf of COSPAR.

or post-processed precise clock provided by the International GNSS Service (IGS) (Johnston et al., 2017) are based on a specific frequency or frequency combination. When using a different frequency or different frequency combination, corrections of DCB/TGD should be applied (Montenbruck and Hauschild, 2013; Montenbruck et al., 2015; Ge et al., 2017).

Using the data of the multi-GNSS experiment (MGEX) network, the institutes of the German Aerospace Center (DLR) and the Chinese Academy of Science (CAS) started to provide intra-frequency DCB products including GPS, GLONASS, BDS, Galileo and QZSS from 2014 (Montenbruck et al., 2015; Wang et al., 2016; Montenbruck et al., 2017). As the IGS precise clock solution is based on a conventional ionosphere-free (IF) combination, i.e., L1/L2 P(Y)-code for GPS, L1/L2 P-code for GLONASS, B1I/B2I for BDS, E1/E5a for Galileo, and L1 C/A and L2C for QZSS (Montenbruck et al., 2015), the clock error for other frequencies or frequency combinations should be corrected by DCB. By comparing the DCB products provided by DLR and CAS, the precision of MGEX DCB is at the level of 0.2–0.6 ns, while monthly stability is within 0.2 ns (Wang et al., 2016).

For real-time navigation application, TGD is usually adopted, which is transmitted in the broadcast navigation message. According to the GNSS interface control document (ICD), the TGD of GPS, Galileo and QZSS refer to the IF combination, while the broadcast clock is based on L1 C/A code for GLONASS. Although GLONASS TGD is not included in a standard receiver independent exchange format (RINEX) navigation file, it is included in the navigation message (Montenbruck et al., 2018). As for BDS, the broadcast clock refers to the B3I frequency. Therefore, BDS-2 provides the TGD corrections TGD_1 and TGD_2, which correct the satellite clock from B3I to B1I and B2I frequency, respectively (CSNO, 2016). These TGD corrections are estimated based on the data from BDS monitoring receivers. Generally, there are two methods to estimate satellite DCB (Li et al., 2014), one is to estimate the DCB simultaneously with global or local ionospheric total electronic content (TEC) modeling, which is adopted at CAS (Li et al., 2012; Wang et al., 2016); another is to estimate from pseudo-range difference after accounting for the ionosphere delay, which is adopted at DLR (Montenbruck et al., 2014). For the TGD estimation at the BDS control segment, the similar strategy of DLR is adopted (Xing et al., 2012).

Although the long-term stability of the estimated BDS TGD is well below 1 ns (Xing et al., 2012), there exists a constant bias between the broadcasted TGD and MGEX DCB provided by IGS for the same frequency or frequency combination (Zhang et al., 2016). This bias makes the assessments of signal-in-space range error (SISRE) using TGD and DCB differ a lot. During a 12-month comparison in 2013–2014, the BDS SISRE shows a better consistency of 1.1 m in RMS after MGEX DCB correction, compared to 1.5 m using broadcast TGD correction (Montenbruck et al., 2015). The performance of single-point positioning also improves when applying MGEX DCB rather than broadcast TGD (Guo et al., 2015). Guo et al. (2015) attribute this to the higher accuracy of MGEX DCB products, while Zhang et al. (2016) further suggest that it comes from the bias in the channel difference between the BDS monitoring station receiver and other commercial receivers. Nevertheless, improving the accuracy of TGD is a continuous challenge in the upgrading of the BDS system.

An apparent update of BDS TGD is observed on July 21, 2017 (Wang et al., 2019), which can be as large as approximately 4.0 ns for TGD_1. However, the origin of this update is unclear, and the impact of this update on user positioning is not assessed. In this contribution, we explain the reason that causes the TGD bias and how the BDS TGD values are updated on July 21, 2017. Section 2 analyzes the pseudo-range data quality of BDS monitoring receivers and explains the motivation for the BDS TGD update. Section 3 gives the detailed updated result of BDS TGD and its difference with MGEX DCB. Then, the impact of the updated TGD on BDS SISRE is compared in Section 4. In Section 5, we analyze the impact of the updated TGD on user positioning regarding single point positioning (SPP) and precise point positioning (PPP) (Zumberge et al., 1997). Finally, conclusions are presented in Section 6.

2. BDS pseudo-range bias

The satellite navigation receiver uses a non-coherent delay locked loop (DLL) to recover the received satellite signals. When the bandwidth of signals is infinite, the accuracy of the pseudo-range measurement can be expressed as (Dierendonck et al., 1992):

$$\sigma_{DLL}^2 = \frac{B_L d}{C/N_0}\left[1 + \frac{1}{(C/N_0)T(1-d)}\right] \quad (1)$$

where σ_{DLL} multiplied by the width of the chip is the standard deviation of pseudo-range measurements expressed in time (s), B_L is the loop bandwidth in Hz, C/N_0 is the carrier noise ratio, T is the accumulated time of correlation processing, and d is the correlation distance after normalization with the width of the code.

From the above equation, we can see that the pseudo-range measurement error can be reduced by reducing the loop bandwidth, extending the signal accumulation time and narrowing the correlation concurrent processing. However, it is easy to lose the lock of the loop by reducing the loop bandwidth, which will reduce the signal acquisition and tracking ability; furthermore, the extending of the signal accumulation time will increase the dynamic stress error. Therefore, narrowing the correlation distance would be a good choice (Tan, 2018). When d = 1/16, compared with d = 1 of regular wide correlation, σ_{DLL} will reduce to 1/4 under the same condition of C/N_0.

To provide a better navigation message, high-accuracy pseudo-range measurements from monitoring receivers

Please cite this article as: Y. Zhang, J. Chen, X. Gong et al., The update of BDS-2 TGD and its impact on positioning, Advances in Space Research, https://doi.org/10.1016/j.asr.2020.03.011

should be used at the BDS measurement control center (MCC). As the BDS MCC adopts a large antenna with an aperture greater than 13 m, its multipath influence is extremely small. The signal transmitted by the user will not be distorted in the satellite transponder (Tan, 2018). Therefore, it is feasible to adopt multiple parallel narrow correlators to obtain a high-accuracy pseudo-range measurement. However, on the other hand, the cost of multiple parallel narrow correlators is quite large. General user receivers usually adopt wide correlators rather than narrow ones, and the accuracy can be guaranteed if there is no distortion in the signal.

The BDS-2 monitoring receivers are able to generate pseudo-range measurements with narrow correlation and wide correlation at B1, B2, and B3 frequencies. As a default setting, the higher accuracy measurements from narrow correlation are adopted for information processing, including orbit determination, TGD and ionosphere parameter estimation.

According to Zhang et al. (2016), a systematic bias was found when comparing BDS-2 broadcast ephemeris with MGEX precise products. It was proved that the bias is quite stable, but different for each satellite. What is more, the bias after ionosphere combination shows a near linear correlation with the values of DCB-minus-TGD. Considering the correlation strategy difference for BDS-2 monitoring receivers and general user receivers, we compare the narrowly correlated and widely correlated pseudo-range measurements at monitoring stations.

For satellite j, the difference at station i is computed by:

$$NW_i^j = average\left(PR_{N,i}^j - PR_{W,i}^j\right) \tag{2}$$

where PR_N and PR_W denote the narrowly correlated and widely correlated pseudo-range measurements.

The difference can be derived at each station. To remove the systematic bias from the receiver hardware delay, we align it to the mean difference of all satellites:

$$dNW_i^j = NW_i^j - \frac{\sum_{j=1}^{n} NW_i^j}{n} \tag{3}$$

Therefore, the difference between the narrowly correlated and widely correlated pseudo-range measurements can be derived on each satellite. Fig. 1 shows the mean value and the STD value of the difference using 9-day data in 2017 obtained from seven monitoring stations. As we can see, there does exist a systematic bias on each satellite with an STD value of less than 0.4 ns, and the bias is different at each frequency. It is clear to see that the bias on B1I is much larger than the other two frequencies, while for the B3I frequency, the bias exhibits the smallest difference. This may due to the larger chip width on B1I signal, which would lead to larger standard deviation of pseudo-range measurement according to Eq. (1). Therefore, larger bias may also occur on B1I signal.

According to the BDS ICD (CSNO, 2016), BDS-2 transmit signals in the frequencies of B1I, B2I, and B3I, and the broadcasted clock correction refers to the frequency at B3I. For the consistency among frequencies, BDS provides TGD_1 and TGD_2 information in navigation messages to correct the satellite clock from B3I to B1I and B2I. Similarly, IGS analysis centers provide a more accurate code bias, i.e., DCB. The relationship between TGD and DCB for BDS can be expressed as (Ge et al., 2017):

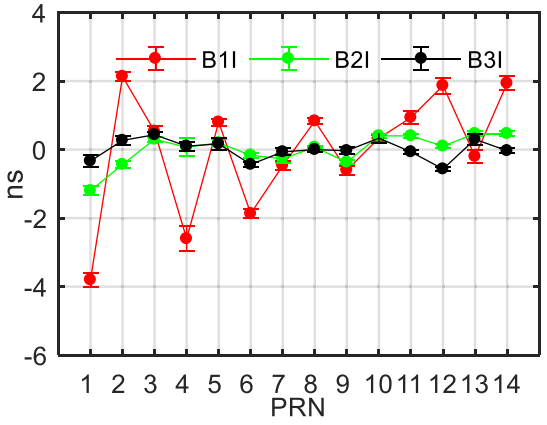

Fig. 1. Difference between the narrowly correlated and widely correlated pseudo-range measurements at BDS-2 monitoring receivers. The error bar stands for standard deviation.

$$\begin{aligned} \mathrm{TGD}_1 &= DCB_{C2I,C6I} \\ \mathrm{TGD}_2 &= DCB_{C7I,C6I} = DCB_{C2I,C6I} - DCB_{C2I,C7I} \end{aligned} \tag{4}$$

where $DCB_{X,Y}$ stands for DCB correction between the observation codes of X and Y. For BDS, the observation codes of C2I, C7I and C6I mean the code observations on B1I, B2I, and B3I. Note that in Eq. (4), the datum bias between TGD and DCB is removed before comparing.

It is proved that there exists a systematic bias between BDS TGD and MGEX DCB (Zhang et al., 2016). To further investigate the relationship between the narrowly correlated and widely correlated pseudo-range bias and the TGD-minus-DCB difference, we use the DCB products provided by CAS (ftp://ftp.gipp.org.cn/product/dcb/mgex/) (Wang et al., 2016) and compare them with BDS TGD. Similar to pseudo-range bias, the TGD-minus-DCB results are aligned to C01. Fig. 2 illustrates the relationship between TGD-minus-DCB and pseudo-range bias. It is interesting to find that the results exhibit a nearly linear relationship with a correlation coefficient of 0.91 for B1I-B3I. For B2I-B3I, the linear relationship is not so significant as the values are all with 1 ns. What is more, the pseudo-range bias seems to have a similar value with TGD-minus-DCB for each satellite. Therefore, we can conclude that the TGD and DCB bias is attributed to the bias of widely correlated and narrowly correlated pseudo-range measurements, as narrowly correlated pseudo-range measurements are adopted at BDS monitoring receivers while the general user receivers at MGEX stations usually adopt the wide correlation technique.

Please cite this article as: Y. Zhang, J. Chen, X. Gong et al., The update of BDS-2 TGD and its impact on positioning, Advances in Space Research, https://doi.org/10.1016/j.asr.2020.03.011

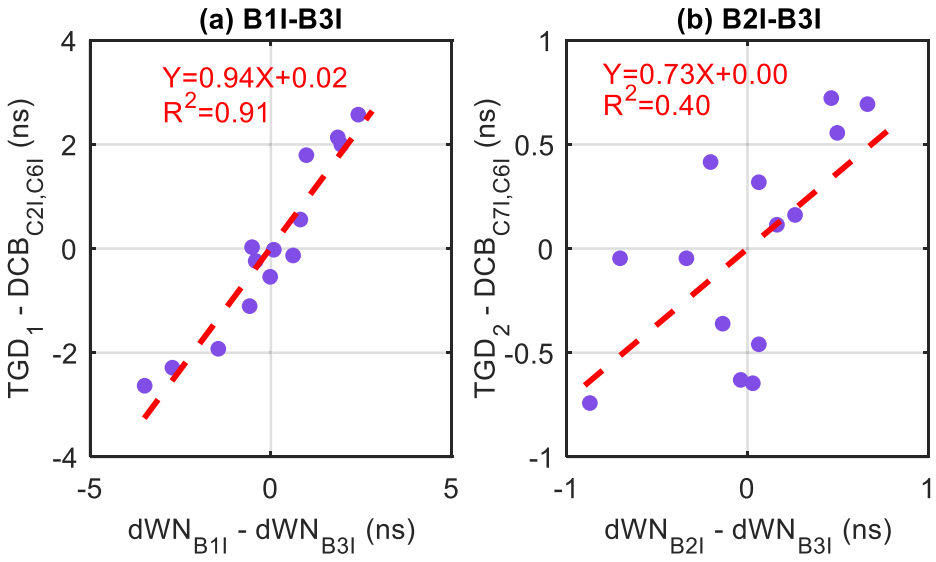

Fig. 2. Relationship between pseudo-range bias and timing group delay (TGD)-minus-differential code bias (DCB) bias. The red dashed line represents the linear fitting function, and R^2 indicates the correlation coefficient. (For interpretation of the references to colour in this figure legend, the reader is referred to the web version of this article.)

3. BDS TGD update

Knowing the fact that a bias does exist between widely correlated and narrowly correlated pseudo-range observations at BDS monitoring receivers and this bias is linear related with the TGD-minus-DCB bias, we decided to adopt the widely correlated pseudo-range measurements rather than narrowly correlated pseudo-range measurements in the BDS control center, including the TGD estimation. On July 21, 2017, a new set of TGDs was uploaded to the BDS broadcast ephemeris and transmitted to users. On July 31, 2017, a set of more precise TGDs was updated using multi-day results.

To illustrate the update of BDS TGDs in 2017, we obtain TGDs from navigation messages and figure out the one-year variation. Fig. 3 shows the TGD values for the existing satellites of BDS in 2017.

It can be observed from Fig. 3 that there were five updates of TGD during the whole year, which is flagged by the dashed line in Fig. 3. For a more detailed view of the update magnitude, the mean differences before and after each update are listed in Table 1. Among the five updates, the updates on January 16, March 13, and May 9 are regular updates of BDS TGD and the difference is within 0.3 ns. Starting from July 21, the widely correlated pseudo-range is used for TGD estimation. Therefore, we can clearly see a significant TGD change on July 21, 2017 from Fig. 3 and Table 1. For instance, the TGD_1 of C02 changes from 5.2 ns to 1.1 ns, and it is from 11.2 ns to 6.4 ns for C14. The mean TGD difference after the update is 2.79 ns for TGD_1 and 0.46 ns for TGD_2, which is equivalent to a 1.88-m difference after IF combination on B1I/B2I, which cannot be neglected. This obvious update on TGD_1 is also observed by Wang et al. (2019). The overall change of TGD_2 after July 21 does not seem obvious compared with TGD_1.

For clarification, the TGD update mentioned below only means the update on July 21, 2017. Meanwhile, the TGD values before and after the update are referred to as old TGD and new TGD to avoid misunderstanding.

For a better understanding of the TGD update, TGD can be compared with the DCB provided by IGS, which shows better accuracy and stability (Wang et al., 2016). By applying Eq. (4) and removing the average TGD-minus-DCB value, TGD is comparable to DCB. Using the weekly MGEX DCB provided by CAS, the difference between TGD and DCB is depicted in Fig. 4.

As can be seen, the difference between TGD_1 and DCB before the update on July 21, 2017, can be as large as 3 ns. After the update, the new TGD_1 difference is well within 1 ns. This kind of improvement is also reported by Wang et al. (2019). As for TGD_2, the difference between old TGD_2 and new TGD_2 is not that significant. For other update epochs of TGD_1 and TGD_2, the change is within the variation amplitude of weekly DCB change.

To further verify the difference between old TGD and new TGD, we calculate the RMS of the mean difference with DCB for each satellite, which is plotted in Fig. 5. Through the comparison, we can figure out that after the TGD update, the TGD difference with DCB for all satellites decreases except C02 on TGD_2, which needs further investigation. The overall difference between BDS TGD and DCB changes from 1.38 ns to 0.29 ns on TGD_1 and from 0.40 ns to 0.25 ns on TGD_2. This indicates that the precision of new TGD is comparable to the accuracy of MGEX DCB products from CAS (Montenbruck et al., 2018).

Please cite this article as: Y. Zhang, J. Chen, X. Gong et al., The update of BDS-2 TGD and its impact on positioning, Advances in Space Research, https://doi.org/10.1016/j.asr.2020.03.011

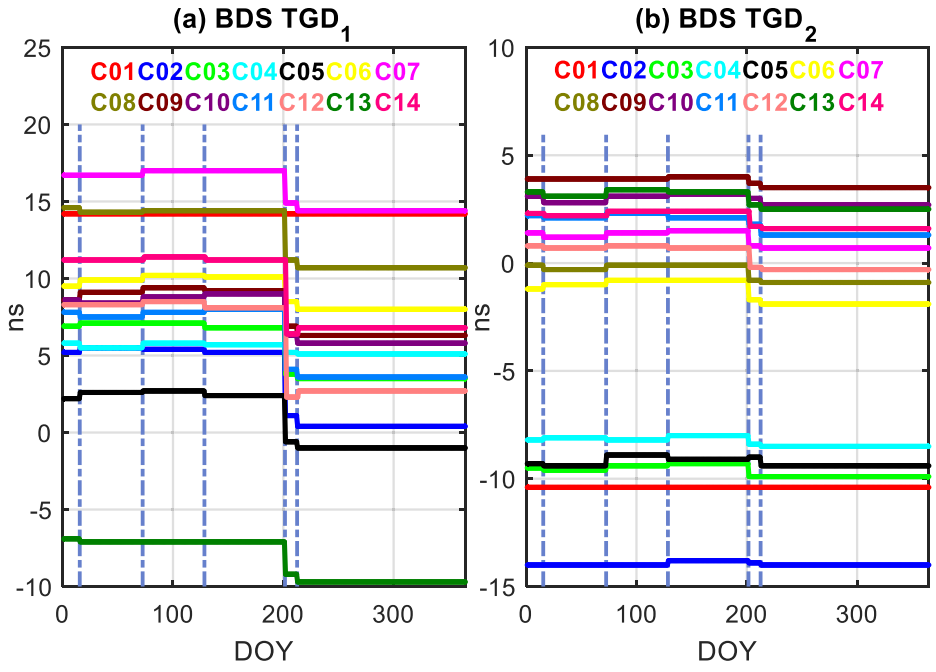

Fig. 3. BDS TGD_1 (a) and TGD_2 (b) variation in 2017. Note that the TGD values of BDS is referred to the B3 signal of C01. The horizontal axis stands for the day of year (DOY), the updated epoch of BDS TGD is marked in a dashed line.

Table 1
BDS-2 TGD updates and the mean difference in 2017.

Update time	Mean TGD_1 difference (ns)	Mean TGD_2 difference (ns)
January 16, 2017	0.22	0.12
March 13, 2017	0.19	0.18
May 9, 2017	0.16	0.10
July 21, 2017	2.79	0.46
July 31, 2017	0.42	0.17

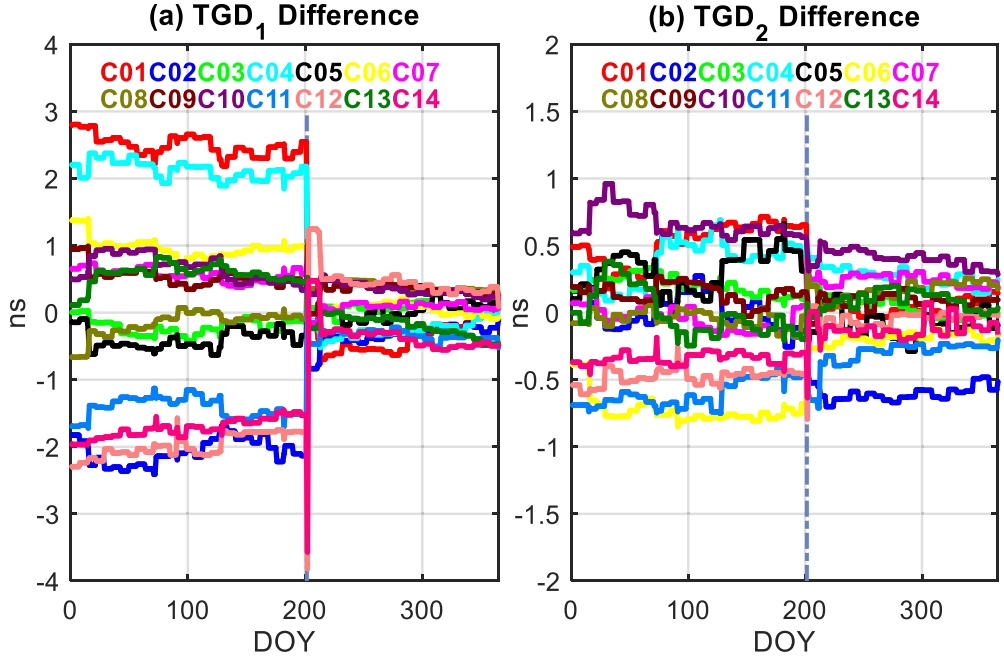

Fig. 4. BDS TGD_1 (a) and TGD_2 (b) difference with multi-global navigation satellite system experiment (MGEX) DCB. The differences between TGD and DCB are normalized to zero-mean values. The dashed line stands for the TGD update on July 21, 2017.

Please cite this article as: Y. Zhang, J. Chen, X. Gong et al., The update of BDS-2 TGD and its impact on positioning, Advances in Space Research, https://doi.org/10.1016/j.asr.2020.03.011

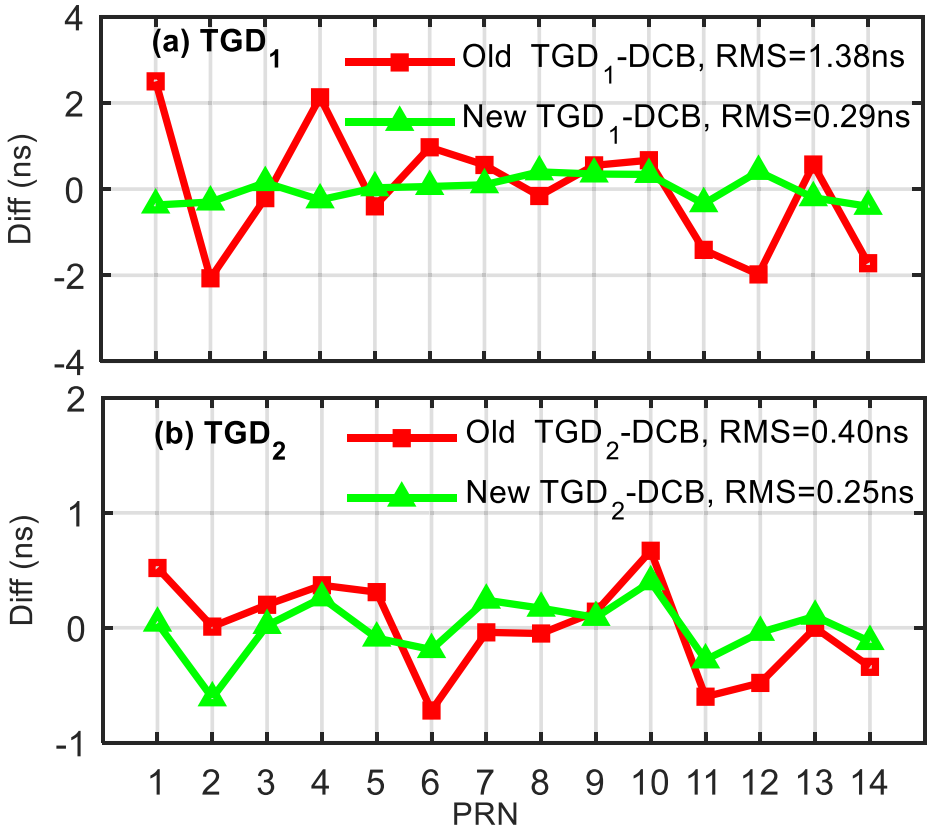

Fig. 5. RMS of BDS TGD_1 (a) and TGD_2 (b) difference with MGEX DCB.

4. TGD update on SISRE

As analyzed by Montenbruck et al. (2015), using MGEX DCB shows a better performance compared with TGD in BDS broadcast SISRE assessment. Considering that SISRE is an important composition of stochastic model in positioning (Kazmierski et al., 2018), it is necessary to assess the SISRE using the updated BDS TGD. By applying the conventional method, the multi-GNSS precise orbit and clock provided by the GeoForschungsZentrum (GFZ), namely "gbm" (Deng et al., 2016), is used for BDS broadcast SISRE assessment.

When comparing broadcast ephemerises with IGS final products, differences in aspects such as time and coordinate system should be considered (Montenbruck et al., 2015). When assessing the SISRE of BDS using gbm products, we should also consider the following corrections:

(1) Satellite antenna offset correction. Starting from January 7, 2017, BDS changed the orbit reference point from the center of mass (CoM) to the antenna phase center (APC) (Wang et al., 2018), which is the same as other GNSS systems. For gbm products, it refers to CoM. Such difference should be corrected when comparing orbit differences. The antenna phase center offset (PCO) used in the broadcast ephemeris is officially released in December 2019 (CSNO, 2019). Meanwhile, for gbm products, PCO values estimated by the European Space Agency (ESA) are adopted (Dilssner et al., 2014). Therefore, the inconsistency of PCO values, which affect clock comparison, should be corrected.

(2) Clock and TGD/DCB correction. It is known that there exists a systematic bias among different products. Commonly, an ensemble clock offset is computed at each epoch from the average broadcast-minus-precise clock values of satellites (Montenbruck et al., 2015). To reduce the effect of gross error from some satellites, we use a medium value of broadcast-minus-precise clock as the offset (Zhang et al., 2016). Meanwhile, the satellite clock in the BDS broadcast ephemeris refers to B3I signal (CSNO, 2016), while for gbm products, it refers to the IF combination of B1I/B2I signal (Deng et al., 2016). This kind of difference between B3I and B1I/B2I should be corrected by TGD.

The TGD correction of the broadcast clock on non-B3I frequencies or other frequency combinations can be expressed as (Ge et al., 2017):

$$\begin{aligned} \mathrm{Corr}_1 &= \mathrm{TGD}_1 \\ \mathrm{Corr}_2 &= \mathrm{TGD}_2 \\ \mathrm{Corr}_{\mathrm{IF12}} &= \frac{f_1^2}{f_1^2-f_2^2}\mathrm{TGD}_1 - \frac{f_2^2}{f_1^2-f_2^2}\mathrm{TGD}_2 \\ \mathrm{Corr}_{\mathrm{IF13}} &= \frac{f_1^2}{f_1^2-f_3^2}\mathrm{TGD}_1 \\ \mathrm{Corr}_{\mathrm{IF23}} &= \frac{f_2^2}{f_2^2-f_3^2}\mathrm{TGD}_2 \end{aligned} \tag{5}$$

Please cite this article as: Y. Zhang, J. Chen, X. Gong et al., The update of BDS-2 TGD and its impact on positioning, Advances in Space Research, https://doi.org/10.1016/j.asr.2020.03.011

where TGD_1 and TGD_2 are the TGD corrections on B1I and B2I from B3I, while f_1, f_2, and f_3 stand for the frequencies of BDS, and IFij (i,j = 1,2,3) means the ionosphere-free combination on frequencies i and j.

When the broadcast clock is corrected to the frequency of the non-B1I/B2I IF combination, the precise clock of gbm products should be corrected to the corresponding frequency using MGEX DCB. The comparison results show that BDS DCB provided by MGEX exhibits a precision of 0.36 ns, while the monthly stability is within 0.17 ns, which satisfies the SISRE evaluation (Montenbruck et al., 2018).

A common method to calculate SISRE can be expressed as (Montenbruck et al., 2015):

$$\mathrm{SISRE} = \begin{cases} \sqrt{(0.99 \cdot R - Clk)^2 + \frac{1}{126}(A+C)^2}, & for\ GEO, IGSO \\ \sqrt{(0.98 \cdot R - Clk)^2 + \frac{1}{54}(A+C)^2}, & for\ MEO \end{cases} \tag{6}$$

where R, A, and C denote the orbit errors in the radial, along-track and cross-track directions, and Clk means the clock error.

To assess the impact of the BDS TGD update on SISRE, one-year data from 2017 are used. The data sampling is set at 15 min, and the threshold of gross outlier rejection is set at 10 m. A monthly SISRE for each satellite is computed except for July, which is divided into two parts, namely before and after the TGD update on July 21, 2017.

In Eq. (6), the contribution of the along-track and cross-track errors on SISRE is relatively small compared with the radial and clock errors. Therefore, we compute the monthly average and STD values of $\alpha \cdot R - Clk$, which contribute to the main part of SISRE. The statistical result of monthly $\alpha \cdot R - Clk$ on the frequency of the B1I/B2I IF combination is shown in Fig. 6, and the corresponding monthly SISRE variation is plotted in Fig. 7. Note that there is no result for C02 in February as gbm products did not provide orbit and clock information for C02 during the whole month of February in 2017.

It can be observed from Fig. 6 that before TGD update on July 21, 2017, there exists a systematic bias for each satellite on $\alpha \cdot R - Clk$, especially for C01, C02, C04, C06, C12, and C14. This is from the bias of the narrowly correlated pseudo-range at BDS monitoring receivers, which can be validated in Fig. 1. When the widely correlated pseudo-range is used and the TGD is updated, the bias reduces to within 1 m. Consequently, a noticeable improvement in

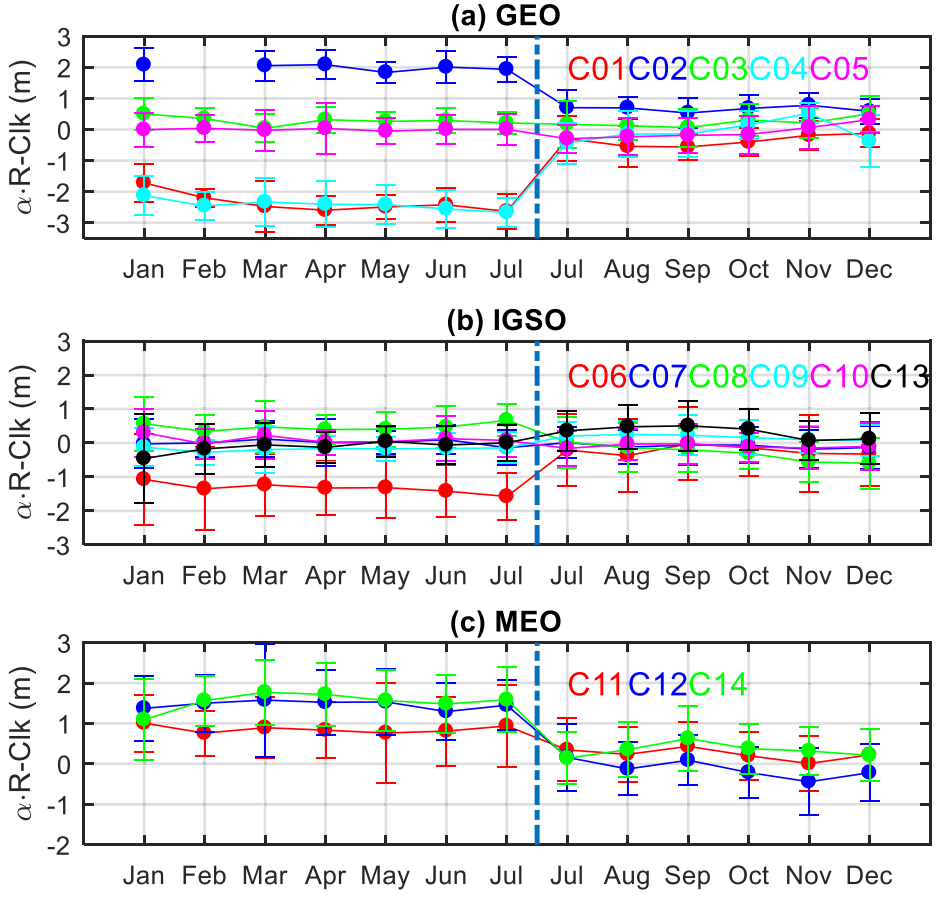

Fig. 6. RMS of monthly BDS $\alpha \cdot R - Clk$ (B1I/B2I) from January to December in 2017 for Geosynchronous Earth Orbit (GEO) (a), Inclined Geosynchronous Orbit (IGSO) (b) and Medium Earth Orbit (MEO) (c) satellites. Note that July is divided into two parts for before and after the TGD update, and the dashed line stands for the TGD update on July 21, 2017.

Please cite this article as: Y. Zhang, J. Chen, X. Gong et al., The update of BDS-2 TGD and its impact on positioning, Advances in Space Research, https://doi.org/10.1016/j.asr.2020.03.011

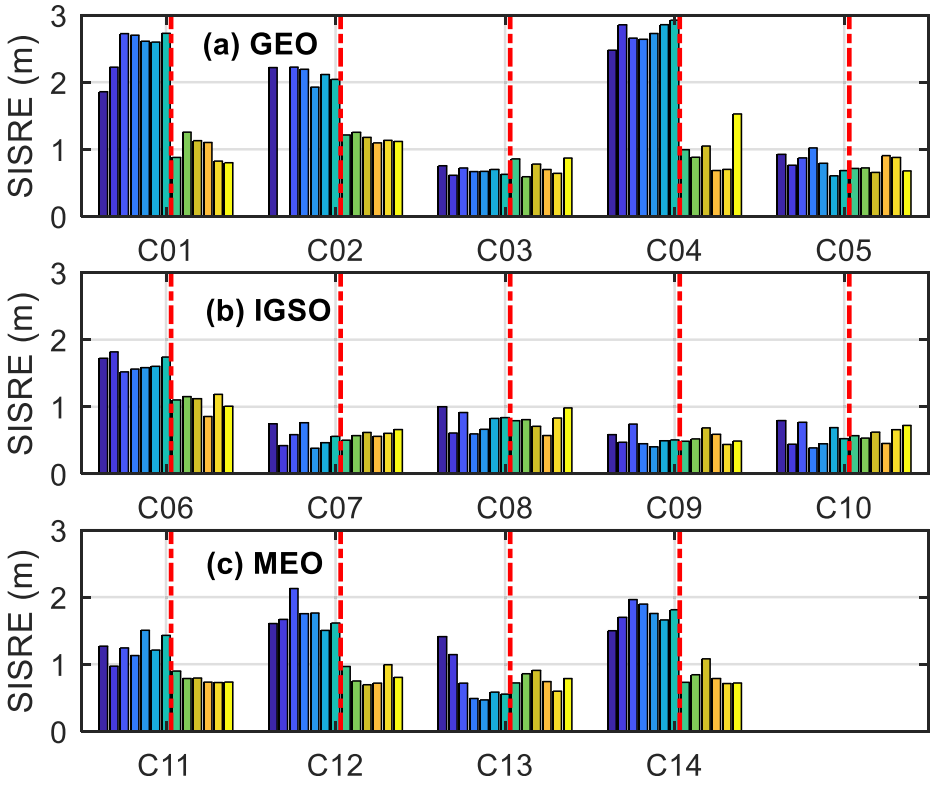

Fig. 7. RMS of monthly BDS signal-in-space range error (SISRE) (B1I/B2I) from January to December in 2017 for GEO (a), IGSO (b) and MEO (c) satellites. Note that July is divided into two parts for before and after the TGD update, and the dashed line stands for the TGD update on July 21, 2017.

SISRE on these satellites is observed from Fig. 7 after the TGD update. This is mainly attributed to the improved accuracy of TGD, as can be seen from Fig. 4. With the new TGD, the SISRE of most satellites could achieve a precision of better than 1 m on the B1I/B2I IF combination.

To fully evaluate the impact of TGD on $\alpha \cdot R - Clk$ and SISRE, monthly average $\alpha \cdot R - Clk$ and SISRE of all satellites on B1I/B2I, B1I, B2I, and B3I are assessed, as shown in Fig. 8. The contribution of the updated TGD to SISRE improvement is much more apparent for the B1I/B2I IF combination compared with other single frequencies. According to Eq. (2), the impact of TGD will be amplified in the IF combination. Thus, the improvement in SISRE on both the B1I/B2I IF and B1I/B3I IF combinations will be more significant. Among different single frequencies, the SISRE improvement on B2I and B3I is not as obvious as on B1I. This is consistent with Fig. 5, where the accuracy improvement of TGD_1 is more significant than TGD_2. Meanwhile, for the SISRE assessment of B3I, it is not affected by the update of TGD in Eq. (2).

To fully compare the impact of the TGD update on SISRE, the old and new TGDs are applied to the same data from DOY 001 to DOY 200 in 2017. The 200-day SISRE statistics of different types of BDS satellites using different TGDs are summarized in Table 2. The overall SISRE improves from 1.33 m to 0.87 m on the B1I/B2I IF combination, while it changes from 1.05 m, 0.92 m, and 0.90 m to around 0.90 m on the B1I, B2I, and B3I frequencies, respectively. Among different satellites on different frequencies, the SISRE of the GEO satellites on the B1I/B2I frequency improves the most. However, the GEO satellites still show the worst SISRE performance compared with IGSO and MEO satellites, which is due to the stationary characteristic of GEO satellites, which suffer from a near-static viewing geometry (Montenbruck et al., 2018). Meanwhile, the SISRE statistics of IGSO satellites are better than those of MEO satellites. This is due to the fact that the BDS monitoring stations are located in China, and MEO satellites cannot be tracked all the time, which will decrease the precision of the broadcasted ephemeris of MEO satellites during a period of few observations or even no observations. Nevertheless, after the TGD update, SISRE statistics on different frequencies are almost the same, which indicates that the new TGD has a similar precision to MGEX DCB values and no longer shows a difference in SISRE assessment.

5. TGD update on user positioning

With the update of TGD values, it is expectable that this would affect the positioning performance on non-B3I frequencies using the broadcasted clock or on non-B1I/B2I

Please cite this article as: Y. Zhang, J. Chen, X. Gong et al., The update of BDS-2 TGD and its impact on positioning, Advances in Space Research, https://doi.org/10.1016/j.asr.2020.03.011

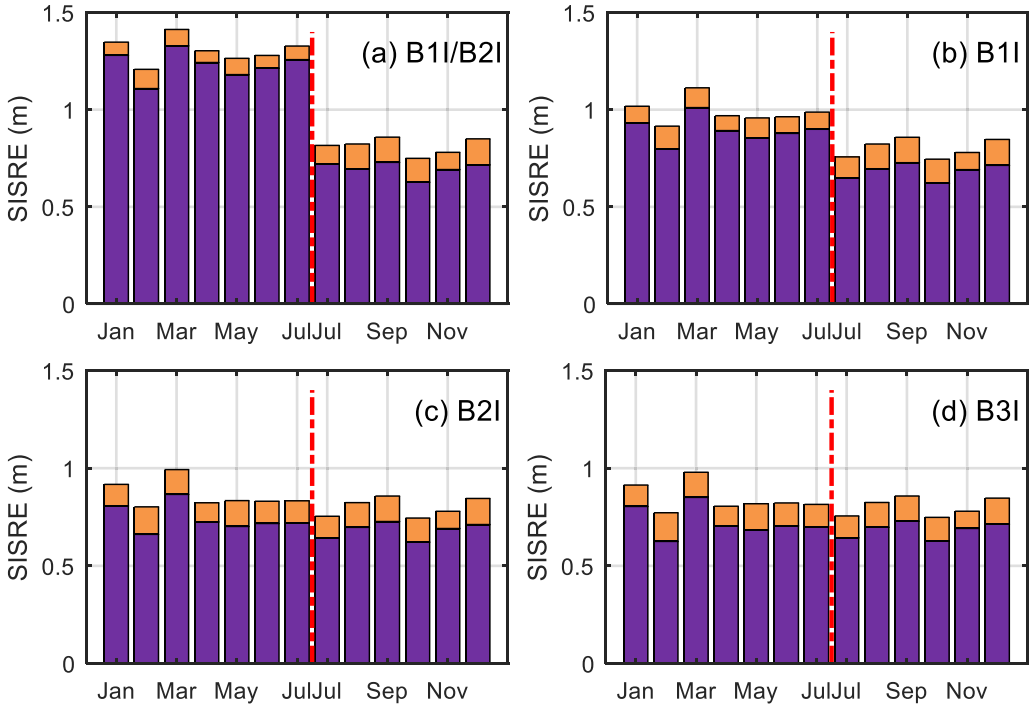

Fig. 8. RMS of monthly BDS $\alpha \cdot R - Clk$ (purple) and SISRE (yellow) from January to December at frequencies of B1I/B2I (a), B1I (b), B2I (c), and B3I (d). Note that July is divided into two parts for before and after the TGD update, and the dashed line stands for the TGD update on July 21, 2017. (For interpretation of the references to colour in this figure legend, the reader is referred to the web version of this article.)

Table 2
BDS SISRE statistics using different TGDs (in meters).

TGD	Frequency	GEO	IGSO	MEO	ALL
Old	B1I/B2I	1.77	0.83	1.58	1.33
	B1I	1.34	0.75	1.16	1.05
	B2I	1.10	0.75	0.96	0.92
	B3I	1.05	0.76	0.92	0.90
New	B1I/B2I	0.93	0.77	0.97	0.87
	B1I	1.00	0.75	0.95	0.89
	B2I	1.08	0.75	0.94	0.91
	B3I	1.05	0.76	0.92	0.90

frequencies using the precise clock. This section investigates the impact of the TGD update on SPP and PPP.

5.1. Data collection and processing strategy

For the assessment of the impact of the TGD update on positioning performance, 28 MGEX stations were selected around Asia-Pacific regions, as shown in Fig. 9. Among these stations, all of them are able to track B1I and B2I data, while 13 of them are able to track triple-frequency data of B1I/B2I/B3I. For a statistical result, one-week data at a sampling rate of 30 s during July 19–25 in 2017 were collected from these stations.

For the processing of SPP and PPP, a homemade software named Net_Diff was used (https://github.com/YizeZhang/Net_Diff), which follows the conventional algorithms of SPP and PPP (Kouba, 2009). The settings of Net_Diff for SPP and PPP are listed in Table 3. For BDS, the estimated parameters are station coordinates and receiver clock in SPP. Meanwhile, for PPP, the residual part of the troposphere delay and carrier phase ambiguities should also be estimated. For coordinate comparison, the reference station coordinates are derived from IGS final solutions.

To assess the impact of the TGD update on SPP and PPP, two sets of TGDs are applied during data processing, i.e., the old TGD and new TGD. Moreover, DCB products provided by CAS are also applied for more comprehensive comparison. Detailed information on correcting TGD/DCB in SPP and PPP can be found in (Guo et al., 2015).

As for the stochastic model of the observations in SPP/PPP, it is composed by:

$$\sigma^2 = \sigma^2_{SISRE} + \sigma^2_{Trop} + \sigma^2_{Iono} + \sigma^2_{Meas}, \quad (7)$$

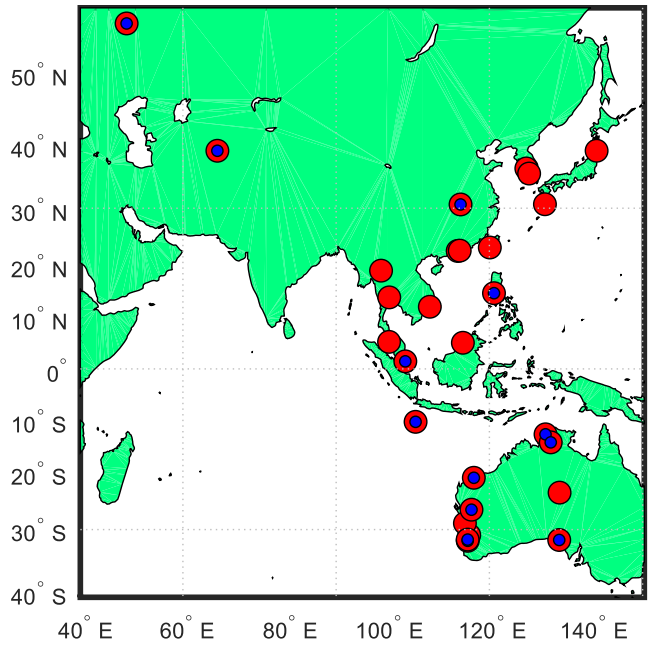

Fig. 9. Twenty-eight selected MGEX stations. The stations able to track B1I/B2I data are marked with a red circle, while stations able to track B1I/B2I/B3I data are marked with a blue circle. (For interpretation of the references to colour in this figure legend, the reader is referred to the web version of this article.)

where σ is the variance of the code observation, while σ_{SISRE}, σ_{Trop}, σ_{Iono}, and σ_{Meas} stand for the SISRE of satellites, troposphere error after model correction, ionosphere error after model correction and the measurement noise of the code or carrier phase, respectively. The settings of each variance are explained in Table 4.

5.2. Single point positioning

Using the Net_Diff software, one-week SPP results of the selected 28 stations are derived. Considering the difference among the old TGD, new TGD and DCB, their impacts on each station are compared in Fig. 10 for B1I/B2I, B1I/B3I, B1I, and B2I. The overall RMS comparison for each component is exhibited in Table 5.

As can be seen from Fig. 10, after the TGD update, the SPP performance on B1I/B2I and B1I/B3I significantly improves at each station, especially in the East component, where the improvement is more than 40%. The overall three-dimensional (3D) improvement for B1I/B2I and B1I/B3I is about 22% after the TGD update, which is higher than that for B1I. This is due to the fact that the ionosphere-free combination amplifies the impact of TGD errors by 2.9 and 3.5 times on B1I/B2I and B1I/B3I. Meanwhile, for B2I SPP, we do not find much difference before and after the TGD update. As we can see from Table 1, the mean difference of TGD_2 change is 0.46 ns, which is small enough considering the variance of code observation. The SPP improvement is comparable to the SISRE improvement analyzed in the previous section. Moreover, we can find that the impact of the new TGD and DCB shows not much difference in SPP performance, which again proves the similar precision of the new TGD and the DCB.

Furthermore, to allow a specific observation of the impact of the TGD update on SPP, we take one of the sta-

Table 3
Settings of single point positioning (SPP)/precise point positioning (PPP) in Net_Diff for BDS.

Option	SPP	PPP
Data sampling	30 s	
Cutoff elevation	10°	
PDOP threshold	10	
Relativistic effects	Corrected (Kouba, 2009)	
Observations	Code	Code + Carrier phase
Troposphere	Zenith: GPT2w (Böhm et al., 2015); Mapping function: VMF1 (Böhm et al., 2015)	Zenith: GPT2w; Mapping function: VMF1Residual part estimated as a random walk parameter. Initial covariance: 0.05 m
Ionosphere	Dual-frequency: Ionosphere-free combinationSingle-frequency: Broadcast ionosphere model	
Satellite phase center offset and variation	Not necessary	Corrected using European space agency (ESA) model (Dilssner et al., 2014)
Satellite orbit and clock	Broadcast ephemeris	Precise product of GBM
Frequency code bias	TGD or DCB	
Receiver phase center offset and variation	Corrected by IGS antenna model (Kouba, 2009)	
Station displacement	Corrected according to IERS 2010 conventions (Petit and Luzum, 2010)	
Phase windup effect	Not necessary	Corrected (Kouba, 2009)
Parameter adjustment	Kalman filter	
Station coordinates	Estimated, white noise for kinematic mode, constant parameter for static mode. Initial variance: 100 m	
Receiver clock	Estimated as white noise. Initial variance: 1 ms	
Ambiguity	Not necessary	Estimated, constant parameter for each arc. Initial variance: 100 m

Table 4
Variance settings of the stochastic model in Net_Diff.

Variance	Settings
σ_{SISRE}	For BDS broadcast ephemeris: 1 mFor precise products: 0.01 m
σ_{Trop}	Zero if the residual part of the troposphere is estimated; Otherwise: $\sigma_{Trop} = \sigma_{Trop\_Z} \cdot mf_{Trop}$,$\sigma_{Trop\_Z}$ is the zenith accuracy of the troposphere model, which is set as 5 cm for GPT2w model (Böhm et al., 2015), and mf_{Trop} is the troposphere mapping function.
σ_{Iono}	Zero if it is an ionosphere-free combination; Otherwise: $\sigma_{Iono} = \sigma_{Iono\_V} \cdot mf_{Iono}$, σ_{Iono_V} is the vertical precision of the ionosphere model correction, which is about 60% of the ionosphere correction for the regional broadcast ionosphere model (Yuan et al., 2019), and mf_{Iono} is the mapping function at the ionosphere pierce point.
σ_{Meas}	Elevation dependent: $\sigma_{Meas} = \left(0.5 + \frac{0.5}{\sin(Ele)}\right)\sigma_0$, Ele is the satellite elevation, and σ_0 is set as 0.3 m for raw code measurement and 0.003 m for raw carrier phase measurement.

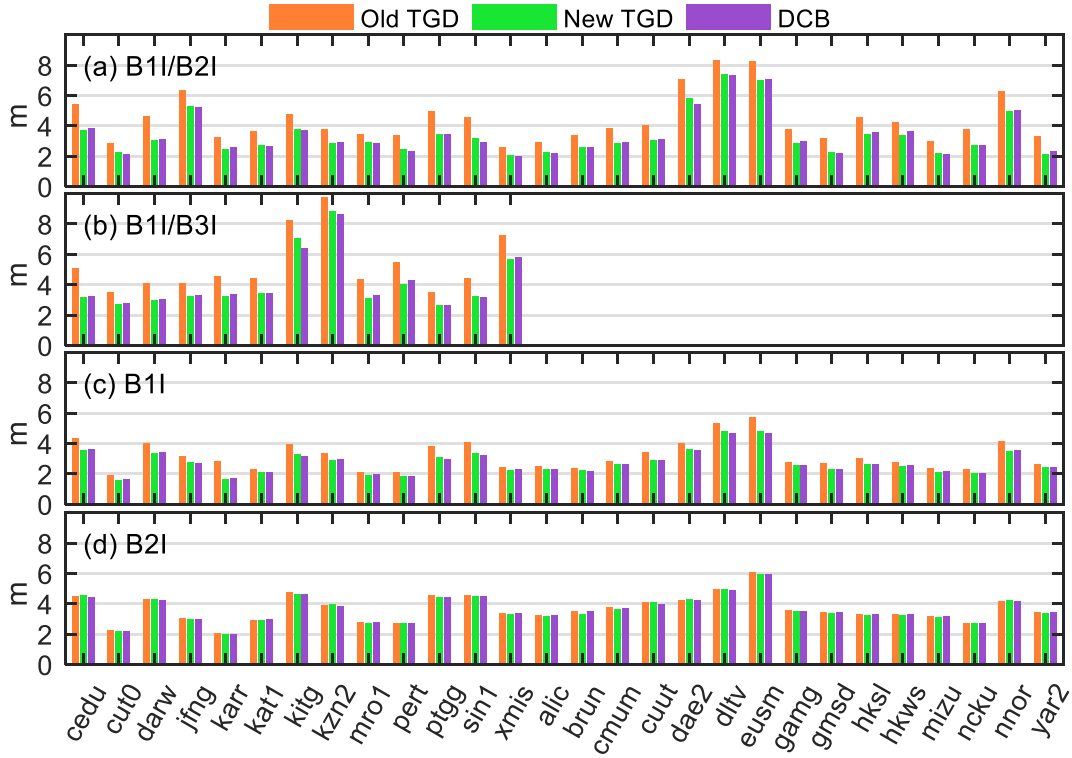

Fig. 10. RMS of BDS SPP 3D positioning performance using different TGDs or DCB on the frequencies of B1I/B2I (a), B1I/B3I (b), B1I (c) and B2I (d), based on one-week data.

tions, JFNG (30.52°N, 114.49°E), as an example. As the DCB and the updated TGD is of the similar precision, it is not compared here. Fig. 11 and Fig. 12 depict the positioning errors in the horizontal and vertical directions for B1I/B2I, B1I/B3I, B1I, and B2I SPP on July 9, 2017. Similarly, it is obvious to see that the positioning errors of B1I/B2I, B1I/B3I and B1I using new TGD are smaller than those using old TGD. Meanwhile, for B2I, not much difference is shown when using new TGD and old TGD. What is more, an obvious non-zero mean bias of positioning error on the horizontal direction for B1I/B2I, B1I/B3I and B1I using old TGD is observed, especially in the East component. When new TGD is applied, this bias almost vanishes.

For further validation, Fig. 13 gives the statistical results of average positioning errors in the North, East, and Up components for all stations on B1I/B2I. It is clear to see the apparent bias in the East component when using old TGD. This explains the significant improvement in SPP RMS in the East component and indicates that the main contribution of the updated TGD is to reduce the systematic bias in the horizontal positioning error. As for the North and Up components, the average positioning error is also more centered at the zero-mean value.

According to Guo et al. (2015) and Chen et al. (2015), the unmodeled errors would be absorbed by the other parameters and positioning residuals. The difference between old TGD and new TGD would also affect the clock parameter and post-fit observation residuals in SPP. Fig. 14 depicts the positioning residuals of SPP on B1I/B2I frequency at station JFNG on July 9, 2017, in

Please cite this article as: Y. Zhang, J. Chen, X. Gong et al., The update of BDS-2 TGD and its impact on positioning, Advances in Space Research, https://doi.org/10.1016/j.asr.2020.03.011

Table 5
RMS and improvement in BDS SPP performance using different TGDs or DCB.

Frequency	TGD/DCB	RMS (m)			Improvement[1](%)			
		North	East	Up	North	East	Up	3D
B1I/B2I	Old TGD	1.59	2.09	3.57				
	New TGD	1.31	1.15	2.93	17.61	44.98	17.93	23.04
	DCB	1.33	1.15	2.91	16.35	44.98	18.49	23.28
B1I/B3I	Old TGD	1.95	2.77	4.2				
	New TGD	1.61	1.65	3.48	17.44	40.43	17.14	22.64
	DCB	1.66	1.61	3.48	14.87	41.88	17.14	22.57
B1I	Old TGD	1.28	1.19	2.63				
	New TGD	1.13	0.8	2.36	11.72	32.77	10.27	13.35
	DCB	1.17	0.78	2.34	8.59	34.45	11.03	13.55
B2I	Old TGD	1.49	0.89	3.24				
	New TGD	1.5	0.88	3.18	−0.67	1.12	1.85	1.39
	DCB	1.49	0.85	3.21	0.00	4.49	0.93	0.98

[1] $Improvement = \left(RMS_{Old\_TGD} - RMS_{New\_TGD/DCB}\right)/RMS_{Old\_TGD}$.

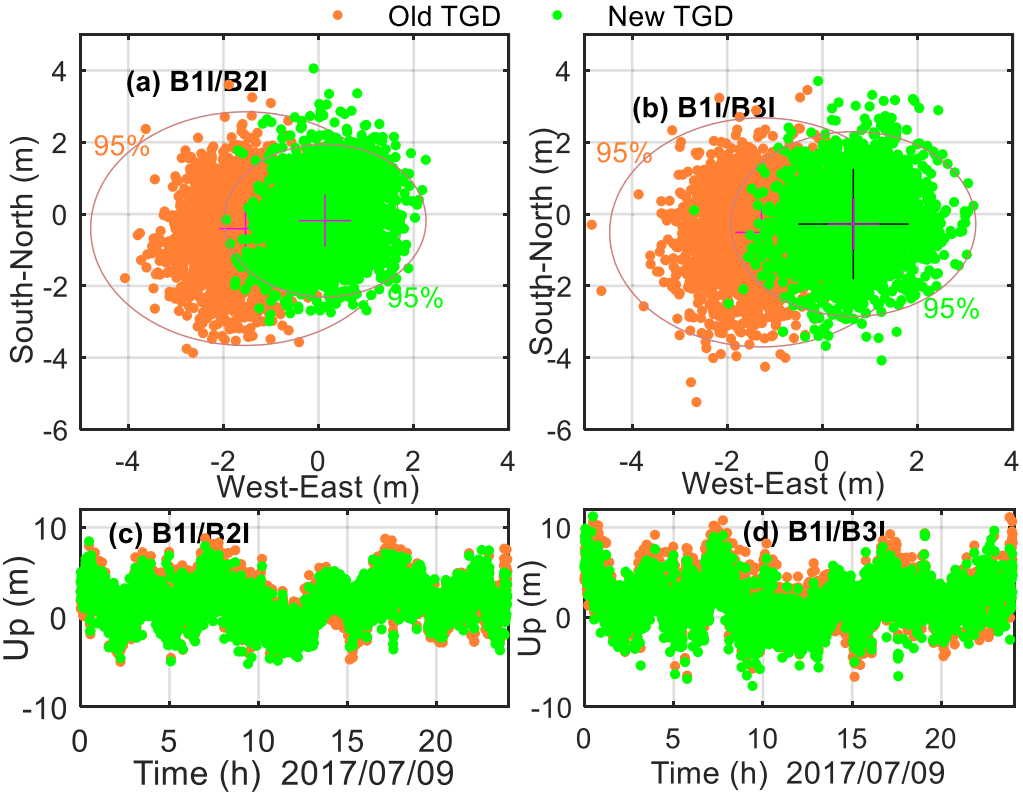

Fig. 11. Horizontal positioning errors of B1I/B2I (a) and B1I/B3I (b) SPP at station JFNG, vertical positioning errors of B1I/B2I (c) and B1I/B3I (d) SPP at station JFNG.

which the code observation is smoothed by the carrier phase to reduce the impact of code observation noise. From the figure, we can also see that bias exists in the positioning residuals for each satellite when using old TGD; this may be attributed to the biased error of old TGD. When new TGD is applied, the level of this bias is reduced. The overall RMS of the residuals also decreases from 1.03 m to 0.73 m. Although it is not shown in this paper, it is expected that the updated TGD will also improve the accuracy of the estimated receiver clock.

5.3. Precise point positioning

As shown in Table 3, the precise orbit and clock provided by gbm are used in PPP, which refers to the B1I/B2I ionosphere-free combination for BDS. Therefore, we

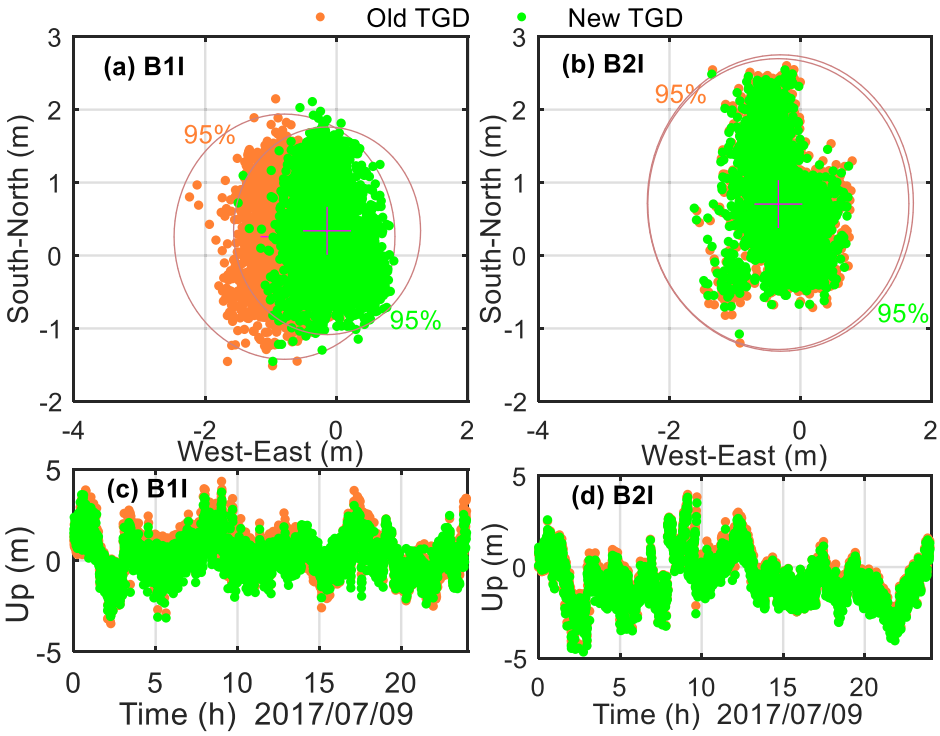

Fig. 12. Horizontal positioning errors of B1I (a) and B2I (b) SPP at station JFNG, vertical positioning errors of B1I (c) and B2I (d) SPP at station JFNG.

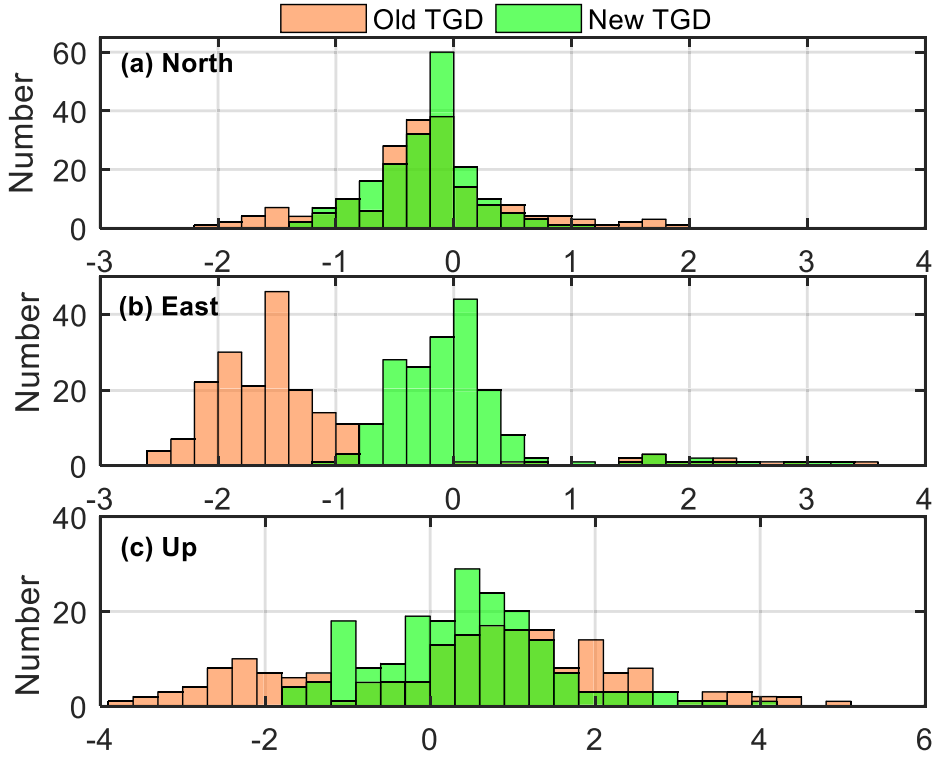

Fig. 13. Statistics of average positioning errors for all stations on B1I/B2I in North (a), East (b) and Up (c) components, using one-week data.

evaluate B1I/B3I-based PPP performance using the old TGD, new TGD and DCB. Note that the inter-frequency clock bias (IFCB) between B1I/B2I and B1I/B3I is not considered in this paper (Li et al., 2017; Pan et al., 2017).

Fig. 15 illustrates the first one-hour B1I/B3I-based BDS PPP performance at station PERT (31.80°S, 115.89°E) on July 12, 2017. As we can see, the update of TGD improves B1I/B3I PPP performance during the convergence period,

Please cite this article as: Y. Zhang, J. Chen, X. Gong et al., The update of BDS-2 TGD and its impact on positioning, Advances in Space Research, https://doi.org/10.1016/j.asr.2020.03.011

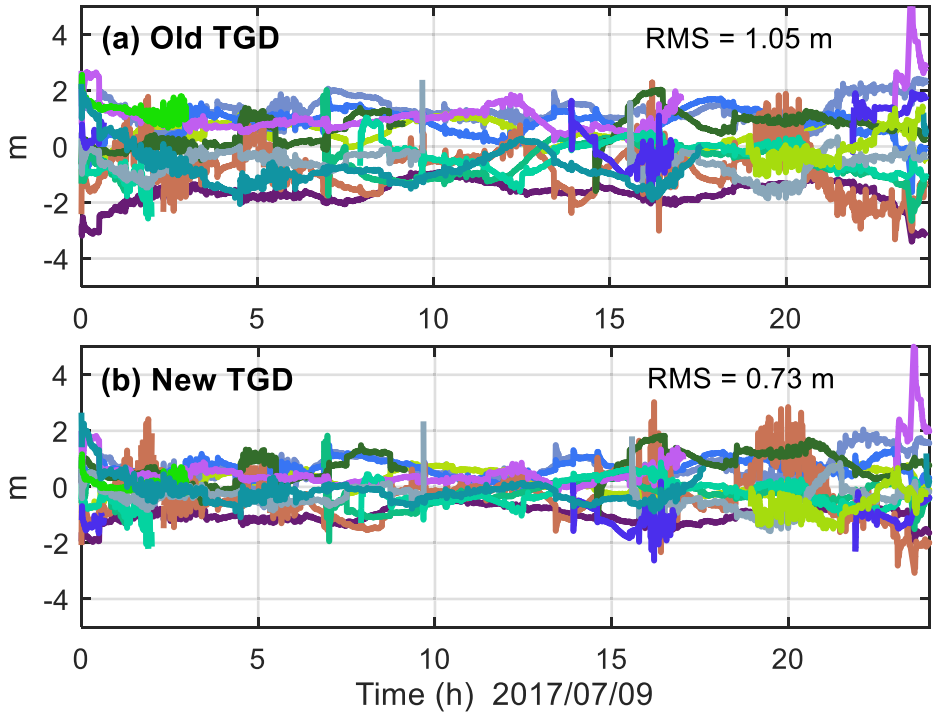

Fig. 14. Smoothed SPP residuals for B1I/B2I SPP using old TGD (a) and new TGD (b) at station JFNG. Different colors stand for different satellites.

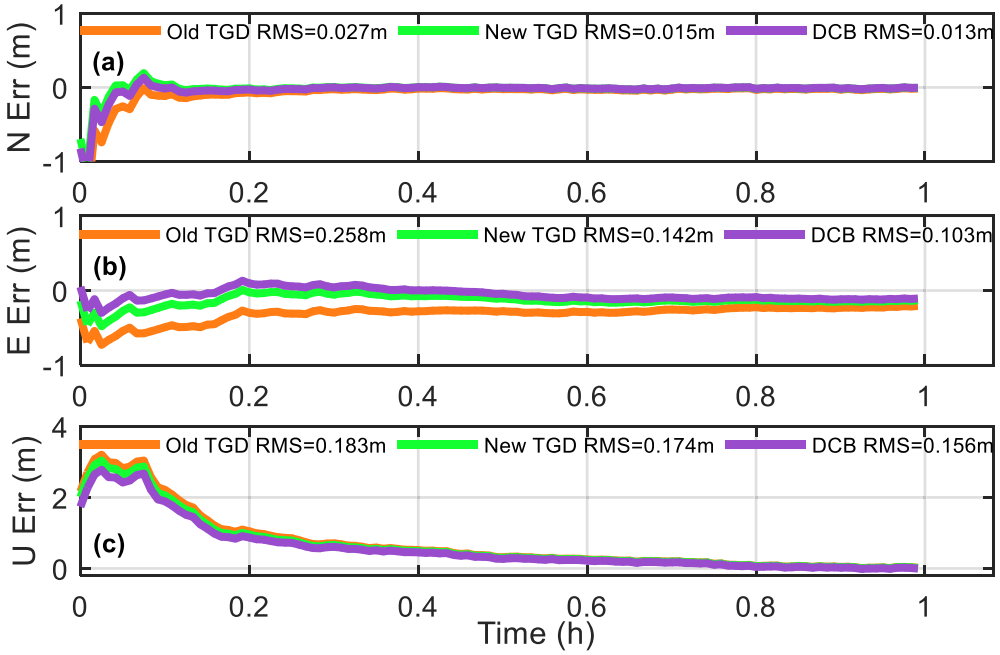

Fig. 15. B1I/B3I-based BDS PPP performance using different TGDs or DCB at station PERT on July 12, 2017.

especially in the East component. With the accumulation of the data, the difference becomes smaller and can be ignored, as TGD only affects code observation, and the positioning precision is less affected by the code observation error with the accumulation of time. For DCB, it seems slightly better than the updated TGD on PPP.

To fully assess the impact of the updated TGD on the convergence performance of B1I/B3I PPP, the data from 13 stations during July 9 and 15, 2017 are processed using the first hour's data on each day. The 3D average positioning errors are plotted every 5 min, as shown in Fig. 16. Similarly, it can be observed that the new TGD improves PPP

Please cite this article as: Y. Zhang, J. Chen, X. Gong et al., The update of BDS-2 TGD and its impact on positioning, Advances in Space Research, https://doi.org/10.1016/j.asr.2020.03.011

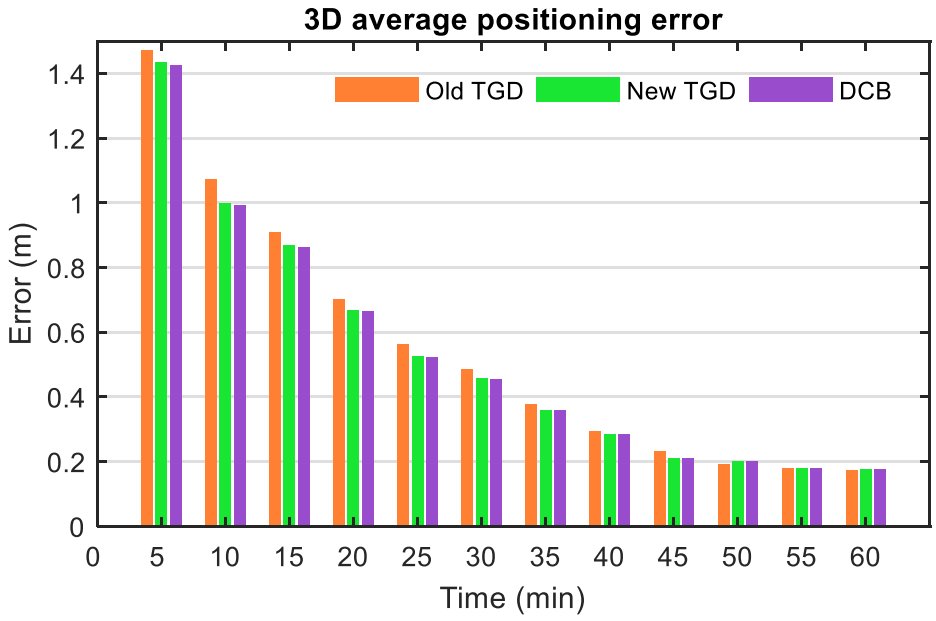

Fig. 16. Statistical B1I/B3I-based BDS PPP convergence performance in the first hour.

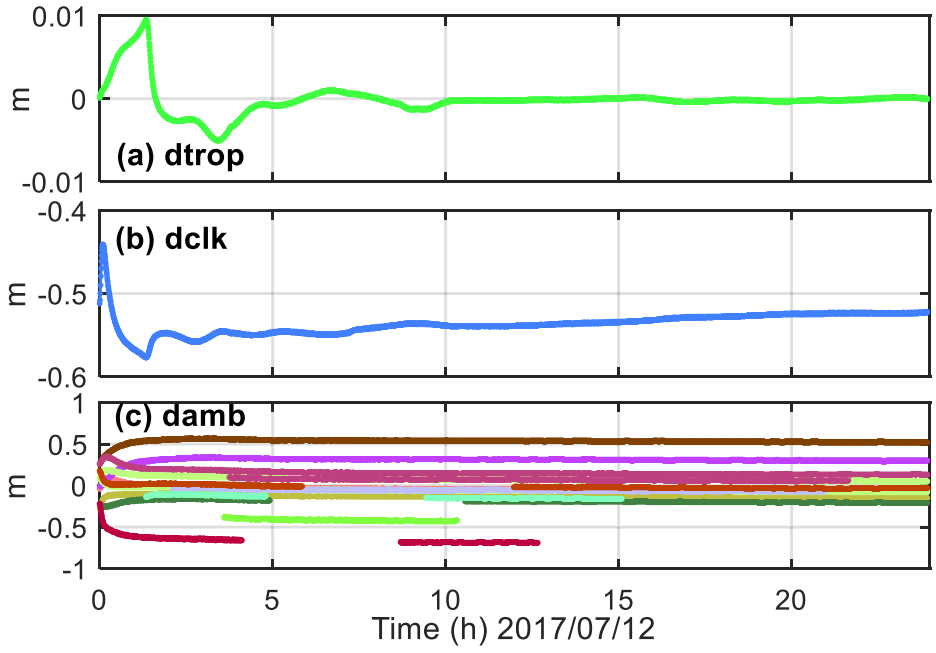

Fig. 17. The difference in the estimated troposphere (a), receiver clock (b) and ambiguity (c) parameters using different TGDs at station PERT on July 12, 2017.

performance during the convergence period, but there seems to be almost no difference after one hour. The improvement in PPP convergence is due to the contribution of the more precise TGD to code measurements, which results in smaller pre-fit code residuals. For DCB, the overall performance is almost the same as the updated TGD.

However, compared with the TGD improvement on SPP, the TGD improvement on PPP is not so significant. To investigate the reason for this in detail, the differences in other estimated parameters including the troposphere, receiver clock, and ambiguities are compared. Fig. 17 depicts the difference at station PERT on July 12, 2017. It is observed that the TGD difference is mostly absorbed by the receiver clock and ambiguities, i.e., the weighted average part of the TGD difference will cause bias in the estimated receiver clock, while the remaining part of the TGD difference at each satellite will cause bias in the estimated ambiguities. As for the troposphere parameter, it is less sensitive to TGD difference, which is also proved by Guo et al. (2015).

Please cite this article as: Y. Zhang, J. Chen, X. Gong et al., The update of BDS-2 TGD and its impact on positioning, Advances in Space Research, https://doi.org/10.1016/j.asr.2020.03.011

6. Conclusions

In this contribution, we investigate the pseudo-range measurements of BDS-2 monitoring receivers and present the bias between widely correlated and narrowly correlated data. The bias shows a linear relationship with BDS TGD-minus-DCB difference, where the DCB from CAS is introduced as reference. Therefore, the BDS-2 control center changed the narrowly correlated pseudo-range into a widely correlated pseudo-range and a new set of TGDs was estimated and updated on July 21, 2017.

A noticeable TGD change with a mean difference of 2.79 ns on TGD_1 and 0.46 ns on TGD_2 is observed after the TGD update. The TGD difference with that provided by MGEX also decrease to 0.29 ns and 0.25 ns, which shows a similar precision with MGEX DCB products from CAS. With the contribution of the updated TGD, the SISRE of BDS in 2017 improves to 0.81 m, showing no difference on each frequency.

The positioning comparison proves that the new TGD will improve SPP performance by about 22% on B1I/B2I and B1I/B3I, mainly from the correction of the biased error in the East component. With a better TGD accuracy, the positioning residuals in SPP also reduce, with a smaller systematic bias. Meanwhile, the updated TGD can also reduce the convergence time of PPP and most of the improved TGD will correct the biased parameters of receiver clock and ambiguity compared with old TGD. Consequently, the update of TGD on July 21, 2017, greatly improved the system performance of BDS and is at the similar precision as DCB.

This paper mainly concentrates on the TGD improvement of BDS-2. With the implementation of BDS-3, it is worth assessing the TGD performance of new BDS-3 satellites and new signals such as B1c and B2a.

Declaration of Competing Interest

The authors declare that they have no known competing financial interests or personal relationships that could have appeared to influence the work reported in this paper.

Acknowledgments

This work is mainly funded by the National Natural Science Foundation of China (No. 11673050); the Key Program of Special Development funds of Zhangjiang National Innovation Demonstration Zone (Grant No. ZJ2018-ZD-009); National Key R&D Program of China (No.2018YFB0504300); and the Key R&D Program of Guangdong province (No.2018B030325001). We thank the IGS for providing GNSS observation data and products, as well as the Chinese Academy of Sciences for the MGEX DCB products.

References

Böhm, J., Möller, G., Schindelegger, M., et al., 2015. Development of an improved empirical model for slant delays in the troposphere (GPT2w). GPS Solut. 19 (3), 433–441.

Chen, J.P., Zhang, Y.Z., Wang, J.X., et al., 2015. A simplified and unified model of multi-GNSS precise point positioning. Adv. Space Res. 55 (1), 125–134.

CSNO, 2016. BeiDou Navigation Satellite System Signal In Space Interface Control Document Open Service Signal (Version 2.1). URL <http://www.beidou.gov.cn/xt/gfxz/201805/P020180507527106075323.pdf>.

CSNO, 2019. Satellite Antenna Phase Center of BDS. URL <http://www.beidou.gov.cn/yw/gfgg/201912/t20191209_19613.html>.

Deng, Z.G., Fritsche, M., Uhlemann, M., et al., 2016. Reprocessing of GFZ multi-GNSS product GBM. In IGS Workshop 2016, Sydney, Australia, 8-12 February.

Dierendonck, V., Fenton, A.J., Ford, P.T., 1992. Theory and performance of narrow correlator spacing in a GPS receiver. Navigation. 39 (3), 265–283.

Dilssner, F., Springer, T., Schönemann, E., et al., 2014. Estimation of satellite antenna phase center corrections for BeiDou. In IGS workshop 2014, California, U.S., June 23-27.

Ge, Y.L., Zhou, F., Sun, B.Q., et al., 2017. The impact of satellite time group delay and inter-frequency differential code bias corrections on multi-GNSS combined positioning. Sensors 17 (3), 602.

Guo, F., Zhang, X.H., Wang, J.L., 2015. Timing group delay and differential code bias corrections for BeiDou positioning. J. Geod. 89 (5), 427–445.

Håkansson, M., Jensen, A.B., Hedling, G., et al., 2017. Review of code and phase biases in multi-GNSS positioning. GPS Solut. 21 (3), 849–860.

Johnston, Gary, Riddell, Anna, Hausler, Grant, 2017. The International GNSS Service. In: Teunissen, Peter J.G., Montenbruck, Oliver (Eds.), Springer Handbook of Global Navigation Satellite Systems. Springer International Publishing, Cham, pp. 967–982.

Kazmierski, K., Hadas, T., Sośnica, K., 2018. Weighting of multi-GNSS observations in real-time precise point positioning. Remote Sens. 10 (1), 84.

Kouba, J., 2009. A guide to using International GNSS Service (IGS) products. URL <https://kb.igs.org/hc/en-us/articles/201271873-A-Guide-to-Using-the-IGS-Products>.

Li, H.J., Li, B.F., Lou, L.Z., et al., 2017. Impact of GPS differential code bias in dual-and triple-frequency positioning and satellite clock estimation. GPS Solut. 21 (3), 897–903.

Li, Z.S., Yuan, Y.B., Li, H., et al., 2012. Two-step method for the determination of the differential code biases of COMPASS satellites. J. Geodesy 86 (11), 1059–1076.

Li, Z.S., Yuan, Y.B., Fan, L., et al., 2014. Determination of the Differential Code Bias for Current BDS Satellites. IEEE Trans. Geosci. Remote Sens. 52 (7), 3968–3979.

Montenbruck, O., Hauschild, A., 2013. Code Biases in Multi-GNSS Point Positioning. Proceedings of the 2013 International Technical Meeting of The Institute of Navigation, San Diego, California, January 2013, pp. 616-628.

Montenbruck, O., Hauschild, A., Steigenberger, P., 2014. Differential code bias estimation using multi-GNSS observations and global ionosphere maps. J. Inst. Navig. 61 (3), 191–201.

Montenbruck, O., Steigenberger, P., Hauschild, A., 2015. Broadcast versus precise ephemerides: a multi-GNSS perspective. GPS Solut. 19 (2), 321–333.

Montenbruck, O., Steigenberger, P., Prange, L., et al., 2017. The Multi-GNSS Experiment (MGEX) of the International GNSS Service (IGS)–achievements, prospects and challenges. Adv. Space Res. 59 (7), 1671–1697.

Please cite this article as: Y. Zhang, J. Chen, X. Gong et al., The update of BDS-2 TGD and its impact on positioning, Advances in Space Research, https://doi.org/10.1016/j.asr.2020.03.011

Montenbruck, O., Steigenberger, P., Hauschild, A., 2018. Multi-GNSS signal-in-space range error assessment–Methodology and results. Adv. Space Res. 61 (12), 3020–3038.

Pan, L., Li, X.X., Zhang, X.H., et al., 2017. Considering inter-frequency clock bias for BDS triple-frequency precise point positioning. Remote Sens. 9 (7), 734.

Petit, G., Luzum, B., 2010. IERS conventions (2010) (No. IERS-TN-36). BUREAU INTERNATIONAL DES POIDS ET MESURES SEVRES (FRANCE). URL <https://www.iers.org/IERS/EN/Publications/TechnicalNotes/tn36.html>.

Tan, S.S., 2018. GNSS systems and engineering: the Chinese Beidou navigation and position location satellite. John Wiley & Sons, Hoboken, USA, pp. 207–208.

Tang, C.P., Hu, X.G., Zhou, S.S., et al., 2018. Initial results of centralized autonomous orbit determination of the new-generation BDS satellites with inter-satellite link measurements. J. Geod. 92 (10), 1155–1169.

Wang, B., Chen, J.P., Wang, B.H., et al., 2018. Signal-in-space Accuracy Analysis for BDS in 2016-2017. In IGS Workshop 2018, Wuhan, China, 29 October-2 November.

Wang, N.B., Yuan, Y.B., Li, Z.S., et al., 2016. Determination of differential code biases with multi-GNSS observations. J. Geod. 90 (3), 209–228.

Wang, N.B., Li, Z.S., Montenbruck, O., et al., 2019. Quality assessment of GPS, Galileo and BeiDou-2/3 satellite broadcast group delays. Adv. Space Res 64 (9), 1764–1779.

Wu, Z.Q., Zhou, S.S., Hu, X.G., et al., 2018. Performance of the BDS3 experimental satellite passive hydrogen maser. GPS Solut. 22 (2), 43.

Xing, N., Wu, X.L., Hu, X.G., et al., 2012. Secular changes in differential code bias of COMPASS system. In: Proceedings of China Satellite Navigation Conference (CSNC) 2012, pp. 243–251.

Yang, Y.X., Li, J.L., Wang, A.B., et al., 2014. Preliminary assessment of the navigation and positioning performance of BeiDou regional navigation satellite system. Sci. China Earth Sci. 57 (1), 144–152.

Yang, Y.X., Xu, Y.Y., Li, J.L., et al., 2018. Progress and performance evaluation of BeiDou global navigation satellite system: Data analysis based on BDS-3 demonstration system. Sci. China Earth Sci. 61, 614–624.

Yang, Y.X., Gao, W.G., Guo, S.R., et al., 2019. Introduction to BeiDou-3 navigation satellite system. Navigation 66 (1), 7–18.

Yuan, Y.B., Wang, N.B., Li, Z.S., et al., 2019. The BeiDou global broadcast ionospheric delay correction model (BDGIM) and its preliminary performance evaluation results. Navigation 66 (1), 1–15.

Zhang, R., Tu, R., Liu, J.H., et al., 2018. Impact of BDS-3 experimental satellites to BDS-2: Service area, precise products, precise positioning. Adv. Space Res. 62 (4), 829–844.

Zhang, Y.Z., Chen, J.P., Zhou, J.H., et al., 2016. Analysis and application of BDS broadcast ephemeris bias. Acta Geodaetica Et Cartographica Sinica. 45 (S2), 64–71.

Zumberge, J.F., Heflin, M.B., Jefferson, D.C., et al., 1997. Precise point positioning for the efficient and robust analysis of GPS data from large networks. J. Geophys. Res.-Sol. EA. 102 (B3), 5005–5017.

Please cite this article as: Y. Zhang, J. Chen, X. Gong et al., The update of BDS-2 TGD and its impact on positioning, Advances in Space Research, https://doi.org/10.1016/j.asr.2020.03.011